AJNR

Fast multiphase MR imaging of aqueductal CSF flow: 2. Study in patients with hydrocephalus.

M Mascalchi, L Ciraolo, M Bucciolini, D Inzitari, G Arnetoli and G Dal Pozzo

AJNR Am J Neuroradiol 1990, 11 (3) 597-603
http://www.ajnr.org/content/11/3/597

Fast Multiphase MR Imaging of Aqueductal CSF Flow: 2. Study in Patients with Hydrocephalus

Mario Mascalchi[1]
Lilina Ciraolo[1]
Marta Bucciolini[1]
Domenico Inzitari[2]
Graziano Arnetoli[2]
Giancarlo Dal Pozzo[1]

The signal intensity in the region corresponding to the cerebral aqueduct was evaluated in three patients with noncommunicating tension hydrocephalus (caused by aqueductal obstruction in two and type I Arnold-Chiari malformation in the other), seven patients with suspected normal-pressure hydrocephalus (three of whom subsequently underwent successful shunting), and 10 patients with ex vacuo (atrophic) hydrocephalus. A gradient-echo MR sequence, called fast multiphase imaging, was used. Serial images corresponding to different phases of the cardiac cycle were acquired. No flow-related enhancement was observed over the entire cardiac cycle in the patients with noncommunicating hydrocephalus. Patients with normal-pressure hydrocephalus showed a higher aqueductal CSF signal intensity, consistent with increased systolic flow rates, than patients with ex vacuo hydrocephalus. When comparing the above two groups of patients with a control group of healthy volunteers, significantly higher and lower values of the (mean) maximum aqueductal signal intensity were found in the normal-pressure hydrocephalus patients and the ex vacuo hydrocephalus patients, respectively.

Fast multiphase MR evaluation of aqueductal CSF flow may help to differentiate patients with different types of hydrocephalus.

***AJNR* 11:597–603, May/June 1990**

Two types of impaired cranial circulation of the CSF implying ventricular dilatation, reversible by a timely neurosurgical shunting procedure, are known. They are called tension and normal-pressure hydrocephalus (NPH), corresponding to the presence or absence of symptoms and signs of increased intracranial pressure [1]. Moreover, the hydrocephalus is said to be communicating or noncommunicating depending on whether or not the ventricular CSF pathway is patent [2].

Another type of hydrocephalus is ex vacuo or atrophic hydrocephalus; this is associated with generalized cortical and subcortical atrophy and is observed in degenerative diseases of the gray matter or as the end stage of white-matter diseases [1]. In the latter condition the shunting procedure, which exposes the patient to a substantial morbidity, is unsuccessful. Cisternographic and clinical physiological studies (e.g., infusion tests) to differentiate NPH from ex vacuo hydrocephalus and to predict a positive outcome to therapeutic ventricular shunting have proved disappointing [3].

Both communicating and noncommunicating hydrocephalus have been the object of an increasing number of studies with MR imaging. MR provides exquisite anatomic details of the patency of the CSF pathway [4–7]. Furthermore, MR can be used to obtain information about CSF flow. Since the aqueduct of Sylvius is the only point of the cranial CSF pathway resembling a conduit, and a considerable amount of experimental work has been devoted to the MR study of flow phenomena in conduits [8–13], particular attention has been paid to the appearance of aqueductal CSF flow, both in normal subjects [14–19] and patients with hydrocephalus [4–7, 15, 20, 21].

In this article we report our early experience with a gradient-echo sequence, fast multiphase imaging (FMI), in the study of tension hydrocephalus, NPH, and ex

Received June 22, 1989; revision requested August 8, 1989; revision received September 28, 1989; accepted October 11, 1989.

Presented in part at the annual meeting of the Society of Magnetic Resonance in Medicine, Amsterdam, August 1989.

This work was supported in part by National Research Council grants 870102002 and 860154502 and the Ministero Pubblica Istruzione.

[1] Department of Clinical Physiopathology, University of Florence, Florence, Italy. Address reprint requests to M. Mascalchi, MR Unit, Radiodiagnostic Section, Department of Clinical Physiopathology, University of Florence, Viale Morgagni 85, 50134 Florence, Italy.

[2] Department of Neurology, University of Florence, Florence, Italy.

0195-6108/90/1103–0597

vacuo hydrocephalus. FMI allows serial images to be obtained of the aqueductal CSF flow within the heart cycle; it is described in detail in a companion article [22].

Subjects and Methods

Three patients with tension hydrocephalus, seven patients with suspected NPH, and 10 patients with atrophic (ex vacuo) hydrocephalus were examined. For comparison, the results obtained in 18 healthy volunteers (11 women and seven men; mean age, 43 ± 13 years) and reported in detail in a companion article [22] were considered.

In two patients, tension hydrocephalus was due to complete aqueductal obstruction; this was demonstrated by 3D spin-echo (SE) sagittal images, 260/30/4 (TR/TE/excitations), which failed to visualize the lumen of the conduit (Fig. 1). One patient, a 30-year-old man, had had viral meningitis at 7 years of age and was diagnosed as having neurosyphilis at the time of examination. The second patient, an 18-year-old woman, had undergone a ventricular shunting procedure for a postinfection aqueductal stenosis 14 months earlier; a shunt dysfunction was suspected at the time of MR examination. The other patient with tension hydrocephalus was a 29-year-old woman with an enlarged head; SE imaging revealed a type I Arnold-Chiari malformation with prominent dilatation of the lateral ventricles. A patent but narrow aqueduct was visualized on 3D 260/30/4 sagittal images. In all three patients, the hydrocephalus was noncommunicating.

NPH was suspected in seven patients (two women and five men; mean age, 61 ± 2 years). At least two of the three clinical features of this condition were present: progressive gait disturbance, mental deterioration and urinary incontinence, and normal lumbar CSF pressure. In addition, at least three of the following CT findings were present: prominent dilatation of the cerebral ventricles, obliteration of the convexity subarachnoid spaces, the presence of periventricular lucencies, and "rounding" of the frontal horns of the lateral ventricles [23]. In one patient (case 2), the CSF laboratory test was positive for syphilis. Another patient (case 6) was a retired boxer. A third patient (case 7), who was hypertensive, had had a transient focal neurologic deficit 4 years before MR. The other four patients had idiopathic NPH. In none of the NPH patients was evidence of obstruction seen within the ventricular CSF pathway on CT; all were considered to have NPH of the communicating type. Four of the NPH patients (cases 1, 3, 6, and 7) subsequently underwent a ventricular shunting procedure. A substantial improvement in the clinical picture was observed in three of them; one (case 6) remained unchanged. In one patient (case 4), increased CSF pressure was seen on continuous intracranial pressure monitoring, but shunting was refused.

The diagnoses in the 10 patients with atrophic hydrocephalus (four women and six men; mean age 63 ± 10 years) were dementia of the Alzheimer type in seven (cases 8–14), vascular dementia in two (cases 15 and 16), and advanced multiple sclerosis in one (case 17). In all these patients, CT revealed prominent cortical atrophy associated with varying degrees of ventriculomegaly.

In the patients with NPH and ex vacuo hydrocephalus, several indexes of ventriculomegaly (bifrontal index, third ventricle index, lateral ventricle index, and biparietal index) [24] were computed. Also, a visual assessment of cortical atrophy, based on the widening of the cortical sulci, was carried out on preliminary conventional axial T1- and T2-weighted SE images; a 0–3 scale was used to grade the atrophy. The results of these evaluations are listed in Table 1.

After a scout sagittal T1-weighted SE image to visualize the aqueductal region, an FMI image [25] in an oblique axial plane through the midportion of the aqueduct was obtained in all patients. The field of view was 250 × 250 mm. On this section a portion of the occipital horns of the lateral ventricles was visualized. The spatial resolution of the FMI images was determined by the matrix size, which was either 256 × 256 or 128 × 128 pixels. The choice of a coarser matrix, allowing halving of the acquisition time, was based on the appearance of a dilated aqueductal lumen on the axial or sagittal SE images. The increased channel size, compensating for the lower spatial resolution, results in negligible partial-volume averaging effects with the periaqueductal gray matter in aqueductal CSF signal sampling. A 256 × 256 matrix was used in the three patients with tension hydrocephalus, three patients with NPH, and four patients with atrophic hydrocephalus. Four NPH patients and six patients with atrophic hydrocephalus were examined with a 128 × 128 matrix.

A 70° flip angle, the shortest trigger delay and echo times (15 msec), and a first-order flow compensation were used. Selecting a heart-phase interval of 50 msec, 18 to 30 serial frames over two cardiac cycles were obtained by dropping every second R wave.

In the patients with NPH and atrophic hydrocephalus, the aqueductal flowing CSF signal intensity was averaged for each consecutive frame, starting from the sixth [22], over a circular region of

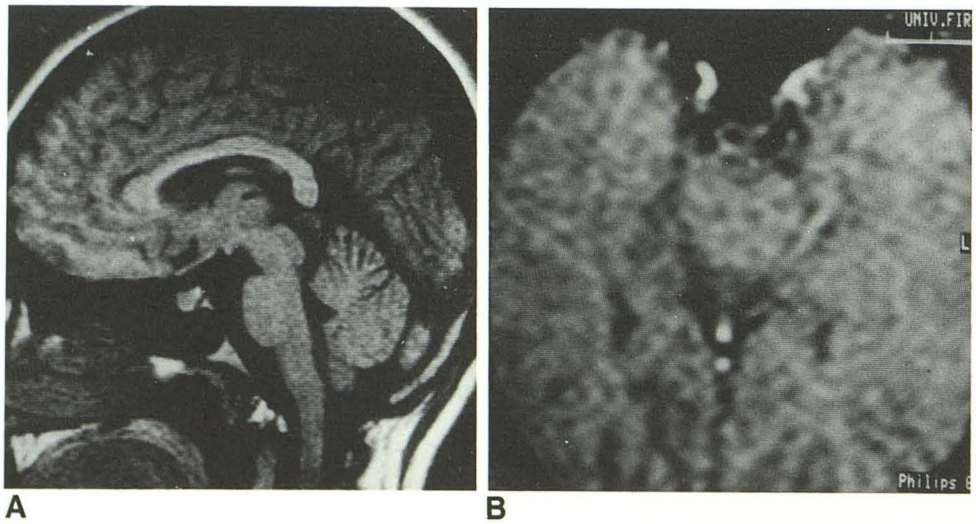

Fig. 1.—Patient operated on for ventriculoperitoneal shunt 14 months before MR examination for tension hydrocephalus.

***A*, Midsagittal 3D spin-echo image, 260/30/4. Aqueductal lumen is not visible, indicating obstruction of conduit.**

***B*, Fast multiphase in oblique axial plane through midportion of aqueductal region corresponding to delay time of 280 msec from R wave. No flow-related enhancement is observed in region of aqueduct, indicating absence of appreciable aqueductal CSF flow.**

TABLE 1: Indexes of Ventriculomegaly, Assessment of Cortical Atrophy, and Maximum and Minimum Ratios of Aqueductal to Lateral Ventricle CSF in Patients with Normal-Pressure Hydrocephalus and Ex Vacuo Hydrocephalus

Group/Case No.	Age (years)	Sex	Index of Ventriculomegaly[a]				Cortical Atrophy[b]	I/Io Ratio[c]	
			Bifrontal	Third Ventricle	Lateral Ventricle	Biparietal		Maximum	Minimum
Normal-pressure hydrocephalus									
1	67	M	0.58	0.08	0.55	0.71	0	4.0	2.2
2	45	M	0.35	0.06	0.35	0.46	0–1	4.4	1.6
3	59	F	0.42	0.10	0.36	0.50	1	6.3	1.6
4	64	M	0.47	0.12	0.37	0.54	0	5.3	1.5
5	66	M	0.42	0.11	0.37	0.60	1	3.4	1.9
6	66	M	0.46	0.13	0.35	0.60	0	4.6	2.9
7	63	F	0.33	0.08	0.35	0.53	1	4.1	1.8
Ex vacuo hydrocephalus									
8	71	F	0.36	0.08	0.34	0.40	2	2.8	1.6
9	68	M	0.33	0.03	0.35	0.48	1–2	2.9	1.9
10	68	M	0.41	0.06	0.35	0.53	1–2	2.5	1.7
11	62	M	0.34	0.07	0.30	0.50	1	3.1	2.1
12	64	M	0.38	0.10	0.37	0.58	2	2.4	1.7
13	56	F	0.45	0.14	0.40	0.50	1	2.4	2.1
14	71	F	0.34	0.04	0.38	0.39	2	2.7	1.6
15	72	F	0.26	0.10	0.30	0.55	2	1.7	1.1
16	58	M	0.36	0.04	0.34	0.50	2	3.2	1.3
17	37	M	0.33	0.04	0.25	0.50	1–2	1.8	1.1

[a] Bifrontal index: ratio of distance between lateral margins of frontal horns to distance between inner table of skull at same level (normal value, 0.37 ± 0.01) [24]; third ventricle index: ratio of distance between lateral margins of third ventricle measured at midportion to distance between inner table of skull at same level (normal value, 0.057 ± 0.003) [24]; lateral ventricle index: ratio of distance between lateral margins of lateral ventricles to distance between inner table of skull at same level (normal value, 0.27 ± 0.01) [24]; biparietal index: ratio of distance between outer margins of posterior horns of lateral ventricles to distance between inner table of skull at same level (normal value, 0.53 ± 0.01) [24].

[b] 0 = absent; 1 = slight; 2 = moderate; 3 = severe.

[c] Rounded to first decimal place. I = aqueductal CSF; Io = lateral ventricle CSF.

interest within the channel cross section. A region of interest of equal size was taken in one of the lateral ventricles, providing a measure of relatively stationary CSF. The behavior of aqueductal and ventricular CSF signal vs the delay time from the R wave was recorded and the curve of the aqueductal/ventricular CSF signal ratio drawn. Differences in the aqueductal/ventricular ratio between the patients with ex vacuo ventriculomegaly or NPH and controls were statistically analyzed using the Student's t test.

Two of the NPH patients who underwent ventricular shunting (cases 6 and 7) were examined again with FMI 4 and 5 months after the operation.

Results

In the two patients with aqueductal obstruction, no flow-related hyperintensity in the region of aqueduct was observed over the entire series of FMI images (Fig. 1). No flow-related enhancement was similarly observed in the patient with type I Arnold-Chiari malformation.

On visual inspection, the signal intensity of the aqueductal CSF consistently appeared very bright in patients with NPH (Fig. 2). In patients with atrophic hydrocephalus, after an initial increase in the first few frames, a progressive decrease was seen in the middle frames; later, a new increase was observed in the last frames (Fig. 3). In both groups the signal intensity findings in the CSF within the lateral ventricles were similar and consistently lower than in the aqueduct.

In both groups, analysis of averaged signal intensity over regions of interest showed the aqueductal signal to vary synchronously with the patient's heart rate, the signal peak occurring with a 280–480-msec delay from the R wave. The signal intensity of the CSF within the lateral ventricles showed minor fluctuations without any heart rate periodicity.

Plots of the aqueductal/ventricular CSF signal ratio vs fractions of heart cycle in one patient with NPH (case 6) and one patient with atrophic hydrocephalus (case 16) are shown in Figure 4. For comparison, the plot of one of the normal volunteers reported in a companion article [22] is shown also. The three curves exhibit similar variations synchronized with the patient's heart cycle but cover different ranges of the aqueductal/ventricular CSF signal ratio.

The maximum (corresponding to systolic phase) and minimum (corresponding to diastolic phase) values of the aqueductal/ventricular CSF signal ratio in each patient with NPH and ex vacuo hydrocephalus are listed in Table 1. The maximum value was observed to be higher in patients with NPH (range, 3.4–6.3) as compared with patients with ex vacuo hydrocephalus (range, 1.7–3.2). On the other hand, the minimum values were similar and overlapped in the two groups.

When comparing the mean aqueductal/ventricular CSF signal ratios of the above groups with that of normal controls [22], significant differences ($p < .001$) in the maximum ratio were found both between patients with NPH (4.6 ± 0.8) and normal subjects (3.2 ± 0.4) and between normal subjects and patients with ex vacuo hydrocephalus (2.5 ± 0.4). The minimum ratio did not differ significantly between the two groups of patients or between either of them and the group of healthy volunteers [22].

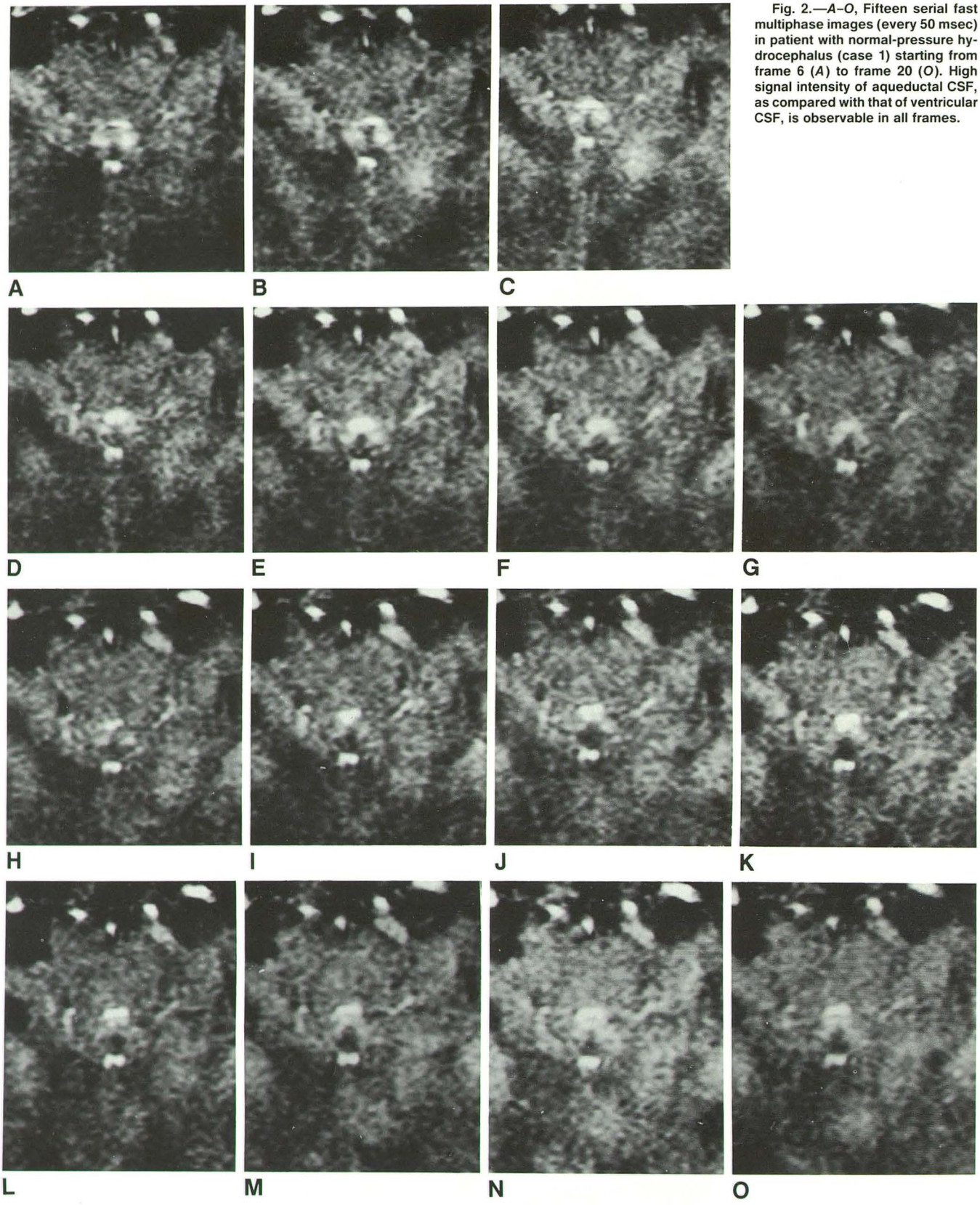

Fig. 2.—*A–O*, Fifteen serial fast multiphase images (every 50 msec) in patient with normal-pressure hydrocephalus (case 1) starting from frame 6 (*A*) to frame 20 (*O*). High signal intensity of aqueductal CSF, as compared with that of ventricular CSF, is observable in all frames.

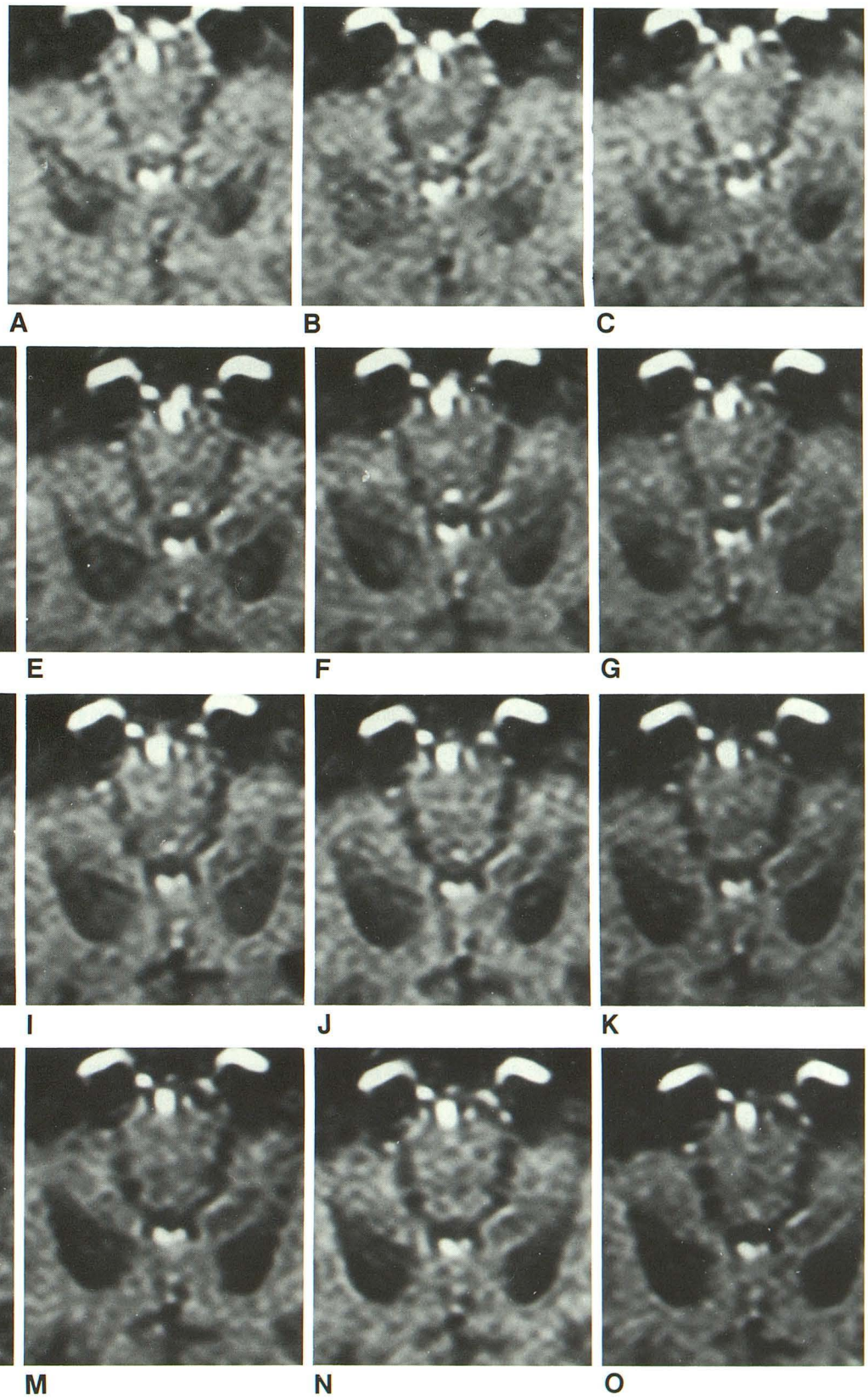

Fig. 3.—*A–O*, Fifteen serial fast multiphase images (every 50 msec) in patient with atrophic hydrocephalus (case 9), starting from frame 6 (*A*) to frame 20 (*O*). Aqueductal CSF signal intensity shows, after initial increase in first few frames, progressive decrease in middle frames; afterward a new increase is observed in last frames.

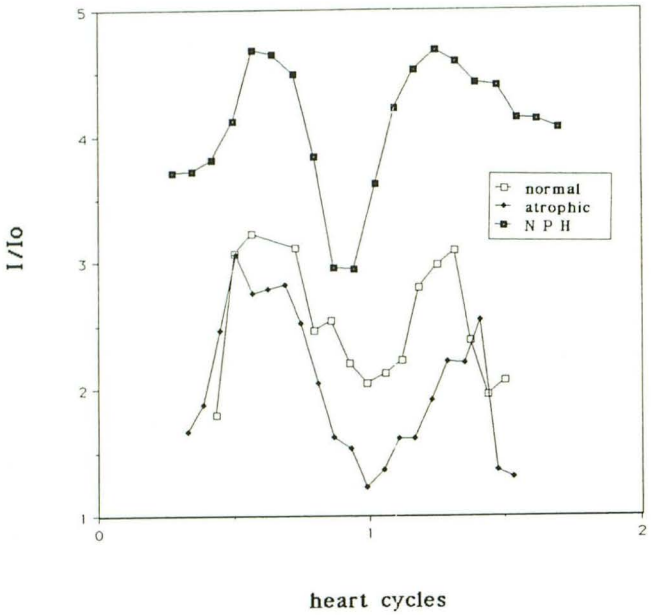

Fig. 4.—Ratio of aqueductal CSF signal (I) to ventricular CSF signal (Io) is plotted vs fractions of heart cycles for a patient with normal-pressure hydrocephalus (NPH) (case 6) and patient with atrophic hydrocephalus (case 16). I/Io ratio for healthy 43-year-old volunteer is plotted for comparison. The three curves, showing similar variations synchronized to heart rate, cover different ranges of I/Io ratio.

In the two NPH patients reexamined by FMI after shunting, decreases were found in both the maximum (from 4.6 to 2.7 in case 6; from 4.1 to 3.8 in case 7) and minimum (from 2.9 to 1.9 in case 6; from 1.8 to 1.7 in case 7) aqueductal/ventricular CSF signal ratios.

Discussion

The superior sensitivity to flow phenomena of gradient-echo imaging as compared with SE imaging [12, 13, 22, 25–27] makes the former particularly suitable for investigation of aqueductal CSF flow. In addition, with FMI the variations in CSF flow that are synchronous with the heart pumping action can be appreciated within acceptable scanning times [22].

Our results, revealing no flow-related enhancement over the cardiac cycle in two cases of aqueductal obstruction, confirm and extend previous studies indicating the capability of MR to provide both anatomic and functional data concerning aqueductal patency [4, 7, 21]. In a further patient with a type I Arnold-Chiari malformation, although a patent aqueduct was visible on sagittal SE images, no flow-related enhancement was observed on FMI. This suggests a condition of decreased or absent flow, presumably due to the anatomic displacement and at least partial obstruction of the foramina of Luschka and Magendie.

To what extent MR is useful in differentiating ex vacuo hydrocephalus from NPH has been debated. In addition to a superior demonstration, as compared with that offered by CT, of the morphologic features of the two conditions, MR, owing to its multiplanarity, allows the evaluation of additional anatomic changes characterizing the two conditions, such as the shape of the third ventricle, the mamillopontine distance, and the corpus callosum modifications [4]. Furthermore, MR can provide a qualitative evaluation of the CSF flow rate, if the flow-related signal modifications, which have been extensively studied in recent years [8–13], are considered. Both time-of-flight and phase-shift effects contribute to the low signal observed in the aqueduct of normal subjects on SE modulus images with no flow compensation. Bradley et al. [15] noted that on SE modulus images with no flow compensation, the signal void within the aqueduct was more pronounced in patients with NPH as compared with healthy subjects. On the other hand, patients with atrophic hydrocephalus had an aqueductal CSF signal intensity significantly higher than that in control subjects. These findings were thought to be consistent with increased and decreased flow rates in NPH and atrophic hydrocephalus, respectively. The usefulness of considering the aqueductal CSF signal intensity for the differentiation of NPH and atrophic hydrocephalus has subsequently been questioned, since a low signal in the aqueduct has been reported in patients with atrophic hydrocephalus also [4, 6, 20].

In gradient-echo imaging, phase-shift effects are smaller than in SE imaging and a flow-related enhancement is observed independent of the flow rate [22]. Although the irregular shape of the conduit, the pulsatility of the flow, and its periodic direction reversal within the cardiac cycle prevent a quantitative evaluation of the aqueductal CSF flow rate [22], we have found that an easily measurable index, that is, the maximum value of the ratio between the FMI signal in the aqueduct to that in the lateral ventricle, may differentiate patients with ex vacuo hydrocephalus and NPH from controls and, more importantly, from each other.

It has to be noted that the patients in our study were diagnosed as having NPH on the basis of clinical and radiologic criteria, which yield a low predictive value regarding the outcome of the shunting procedure [3, 28, 29]. By using these criteria, an unsuccessful shunting procedure could actually be due to either a misdiagnosis or an arrested hydrocephalus. In three of our four patients who were operated on, the outcome of the shunting procedure was successful, confirming the diagnosis of NPH.

The mechanisms implying increased and decreased flow rates in NPH and atrophic hydrocephalus have been discussed elsewhere [15]. We only wish to stress that intracranial pressure monitoring studies reveal that CSF pressure is not "normal" in NPH patients successfully shunted; this is true of both resting pressure and the frequency and amplitude of the high-pressure waves [30–32]. These elevations in intracranial pressure could imply increased pressure gradients along the CSF pathway, and hence increased aqueductal CSF flow rates.

Interestingly, in the two NPH patients in our series examined after surgery, lower aqueductal CSF flow enhancement was found on FMI, as compared with that observed preoperatively. This finding, consistent with decreased flow rates, is in agreement with the lowering of the intracranial pressure

recorded in intracranial pressure studies after shunting operations [31].

Obviously, our observations need to be confirmed by further studies in a larger sample size before information on aqueductal CSF flow rate provided by gradient-echo MR can be used advantageously in the evaluation of patients with hydrocephalus.

ACKNOWLEDGMENTS

We thank Massimo Baroni and Loriana Bendoni for technical assistance.

REFERENCES

1. Adams RD, Victor M. Disturbances of cerebrospinal fluid circulation, including hydrocephalus and meningeal reactions. In: Adams RD, Victor M, eds. *Principles of neurology*. New York: McGraw-Hill, **1989**:501–515
2. Dandy WE. Experimental hydrocephalus. *Ann Surg* **1919**;70:129
3. Huckman MS. Normal pressure hydrocephalus: evaluation of diagnostic and prognostic tests. *AJNR* **1981**;2:385–395
4. El Gammal, Allen MB, Brooks BS, Mark K. MR evaluation of hydrocephalus. *AJNR* **1987**;8:591–597
5. Kemp SS, Zimmermann RA, Bilaniuk LT, Hackney DB, Goldberg HI, Grossman RI. Magnetic resonance imaging of the cerebral aqueduct. *Neuroradiology* **1987**;29:430–436
6. Jack CR, Mokri B, Laws ER, Houser OW, Baker HL, Petersen RC. MR findings in normal pressure hydrocephalus: significance and comparison with other forms of dementia. *J Comput Assist Tomogr* **1987**;11:923–931
7. Atlas SW, Mark AS, Fram EK. Aqueductal stenosis: evaluation with gradient echo rapid MR imaging. *Radiology* **1988**;169:449–453
8. Axel L. Blood flow effects in magnetic resonance imaging. *AJR* **1984**;143:1157–1166
9. Bryant DJ, Payne JA, Firmin DN, Longmore DB. Measurement of flow with NMR imaging using a gradient pulse and phase difference technique. *J Comput Assist Tomogr* **1984**;8:588–593
10. Bradley WG Jr, Waluch V. BLood flow: magnetic resonance imaging. *Radiology* **1985**;154:443–450
11. Malko JA, Hoffman JC Jr, McClees EC, Davis PC, Braun IF. A phantom study of intracranial CSF signal loss due to pulsatile motion. *AJNR* **1988**;9:83–89
12. Evans AI, Hedlund LW, Herfkens RI, Utz IA, Fram EK, Blindes RA. Evaluation of steady and pulsatile flow with dynamic MRI using limited flip angles and gradient refocused echoes. *Magn Reson Imaging* **1987**;5:475–482
13. Gao JH, Holland SK, Gore JC. Nuclear magnetic resonance imaging signal from flowing nuclei in rapid imaging using gradient echoes. *Med Phys* **1988**;15:809–914
14. Sherman JL, Citrin CM. Magnetic resonance demonstration of normal CSF flow. *AJNR* **1986**;7:3–6
15. Bradley WG Jr, Kortman KE, Burgoyne B. Flowing cerebrospinal fluid in normal and hydrocephalic states: appearance on MR images. *Radiology* **1986**;159:611–616
16. Bergstrand G, Bergstrom M, Nordell B, et al. Cardiac gated MR imaging of cerebrospinal fluid flow. *J Comput Assist Tomogr* **1985**;9:1003–1006
17. Citrin CM, Sherman JL, Gangarosa RE, Scanlon D. Physiology of the CSF flow-void sign: modification by cardiac gating. *AJNR* **1986**;7:1021–1024
18. Mark AS, Feinberg DA, Brant-Zawadzki MN. Changes in size and magnetic resonance signal intensity of the cerebral CSF spaces during the cardia cycle as studied by gated, high resolution magnetic resonance imaging. *Invest Radiol* **1987**;22:290–297
19. Mascalchi M, Ciraolo L, Tanfani G, et al. Cardiac-gated phase MR imaging of the aqueductal CSF flow. *J Comput Assist Tomogr* **1988**;12:923–926
20. Sherman JL, Citrin CM, Gangarosa RE, Bowen BJ. The MR appearance of CSF flow in patients with ventriculomegaly. *AJNR* **1986**;7:1025–1031
21. Njemanze PC, Beck OJ. MR-gated intracranial CSF dynamics: evaluation of pulsatile CSF flow. *AJNR* **1989**;10:77–80
22. Ciraolo L, Mascalchi M, Bucciolini M, Dal Pozzo G. Fast multiphase MR imaging of the aqueductal CSF flow: 1. Study of healthy subjects. *AJNR* **1990**;11:589–596
23. Vassilouthis J. The syndrome of normal pressure hydrocephalus. *J Neurosurg* **1984**;61:501–509
24. Leys D, Pruvo JP, Petit H, Gaudet Y, Clarisse J. Maladie D'Alzheimer. Analyse statistique des resultats du scanner X. *Rev Neurol* (Paris) **1989**;145:134–139
25. Van Dijk P. Multiphase mode and cinedisplay permit dynamic flow MR imaging. *Diagn Imaging* **1986**;10:163–168
26. van der Meulen P, Groen JP, Cuppen JJM. Very fast MR imaging by field echoes and small angle excitations. *Magn Reson Imaging* **1985**;3:297–299
27. Frahm I, Haase A, Matthaei D. Rapid NMR imaging of dynamic processes using the FLASH technique. *Magn Reson Med* **1986**;3:321–327
28. Anonymous. Cerebral atrophy or hydrocephalus? (editorial) *Br Med J* **1980**;285:348–349
29. Anderson M. Normal pressure hydrocephalus. *Br Med J* **1986**;293:837–838
30. Symon L, Dorsh NWC, Stephens RC. Pressure waves in so called normal pressure hydrocephalus. *Lancet* **1972**;2:1291–1292
31. Symon L, Dorsh NWC. Use of the long term intracranial pressure measurement to assess hydrocephalic patients prior to shunt surgery. *J Neurosurg* **1975**;42:258–273
32. Pappadá G, Poletti C, Guazzoni A, Sani R, Colli M. Normal pressure hydrocephalus: relationship among clinical picture, CT scan and intracranial pressure monitoring. *J Neurosurg Sci* **1986**;30:115–121